Analytical Investigation of the Dynamics

of Tethered Constellations in Earth Orbit (Phase II)

Principal Investigator

Dr. Enrico C. Lorenzini

March 1986

+---+
| The Smithsonian Astrophysical Observatory |
| is a member of the |
| Harvard-Smithsonian Center for Astrophysics |
+---+

Analytical Investigation of the Dynamics

of Tethered Constellations in Earth Orbit (Phase II)

Contract NAS8-36606

Quarterly Report #4

For the period 22 December 1985 through 21 March 1986

Principal Investigator
Dr. Enrico C. Lorenzini

Co-Investigators
Mr. David A. Arnold
Dr. Mario D. Grossi
Dr. Gordon E. Gullahorn

March 1986

CONTENTS

Abstract

The "g-tuning" maneuvers of a 3-mass, vertical tethered system are dealt with in this quarterly report. In particular, the case of reaching a zero-g acceleration level on board the middle mass from a non-zero initial condition is analyzed. A control law that provides a satisfactory transient response is derived.

The constellation dynamics in the case of the middle mass travelling from one tether tip to the other is also investigated. Instabilities that take place at the end of the maneuver are analyzed and accommodated by devising suitable damping algorithms.

1,2

Figure Captions

Figure 2.1.1   Geometry of the 3-mass tethered system at the

beginning and at the end of the "zero-g-tuning" maneuver.

Figure 2.1.2 a-i   Dynamic response of the 3-mass tethered system during

a transfer maneuver, along the tether, of the middle

mass from the Space Station to the system C.M.

("zero-g-tuning" maneuver).

Figure 2.2.1 a-m   Dynamic response of the 3-mass tethered system

during a transfer maneuver, along the tether, of the

middle mass from the Space Station to the opposite

tether end.

Figure 2.2.2   Tether tension vs. time in tether #2 in the case of

the transfer maneuver of the middle mass from the Space

Station to the opposite tether end. The tension

profile obtained by adopting an adaptive control logic

is compared to the non-adaptive control strategy.

1.0 INTRODUCTION

This is the fourth quarterly report submitted by SAO under contract NAS8-36606, "Analytical Investigation of the Dynamics of Tethered Constellations in Earth Orbit (Phase II)," Dr. Enrico Lorenzini, PI. This report covers the period from 22 December 1985 through 21 March 1986.

2.0 TECHNICAL ACTIVITY DURING REPORTING PERIOD AND PROGRAM STATUS

2.1 A Particular Case Of "G-Tuning." Reaching The Zero-G Acceleration Condition On The Middle Mass.

The analysis of "g-tuning" in the 3-mass, vertical tethered system was started in Quarterly Report #3. In that report two different cases of "g-tuning" were analyzed in order to devise a control law that gives a satisfactory transient response. More simulations have been performed during this reporting period aimed at improving the transient response during the maneuver. The particular case of "g-tuning" that has been recently investigated is related to the achievement of zero-g acceleration condition on board the middle mass starting from a non-zero acceleration initial condition.

Since the gravity gradient field is linearized in our present computer code, the zero-g point coincides with the system C.M. The maneuver described in this section starts with the middle platform placed 10 m away from the reeling mechanisms on the Space Station. Subsequently the platform is moved toward the C.M. position of the system pertaining to the final configuration of the constellation. The middle mass, therefore, has to reach the final C.M. position with zero velocity and zero acceleration. For this simulation the modified

hyperbolic tangent control law adopted in Quarterly Report #3 for the "g-tuning" (equations 2.6.1) has been improved. That control law has been further modified in order to have a slower acceleration phase at the beginning of the maneuver. The new control law is therefore as follows:

$$\ell_1 = \ell_{10} + \Delta\ell_c \left[\tanh(\alpha t)\right]^\gamma$$
$$\ell_2 = \ell_{20} - \Delta\ell_c \left[\tanh(\alpha t)\right]^\gamma \qquad (2.1.1)$$

The exponent $\gamma > 1$ slows down the acceleration phase and speeds up the deceleration phase. The net result is very positive since the previous control law had a too rapid acceleration phase and a too slow deceleration phase. In the simulation, shown later on, $\alpha = 1/1000$ sec^{-1} and $\gamma = 4$ have been adopted. The position of the system C.M. at the end of the maneuver is estimated beforehand in order to compute $\Delta\ell_c$. With reference to Figure 2.1.1, $\Delta\ell_c$ is given by:

$$\Delta\ell_c = \frac{\ell_{CM1f} - \ell_{c10}\ (1 + 2\ T_{1f}/EA)}{1 + 2\ T_{1f}/(EA)} \qquad (2.1.2)$$

where ℓ_{CM1f} is the distance of the system C.M. from m_1 at the end of the maneuver, ℓ_{c10} is the initial controlled tether #1 length and T_{1f} is the final tension in tether #1.

We also have:

$$\ell_{CM1f} = \ell_{tot,f}\ m_3/(m_1 + m_3) \qquad (2.1.3)$$

$$\ell_{tot,f} = \frac{\ell_{c10} + \ell_{c20}}{1 + (\ell_{c10} + \ell_{c20})\,6\Omega^2 m_{eq1,3}/(EA)} \qquad (2.1.4)$$

where $\ell_{tot,f}$ is the overall constellation length at the end of the maneuver and

Initial Stage   Final Stage
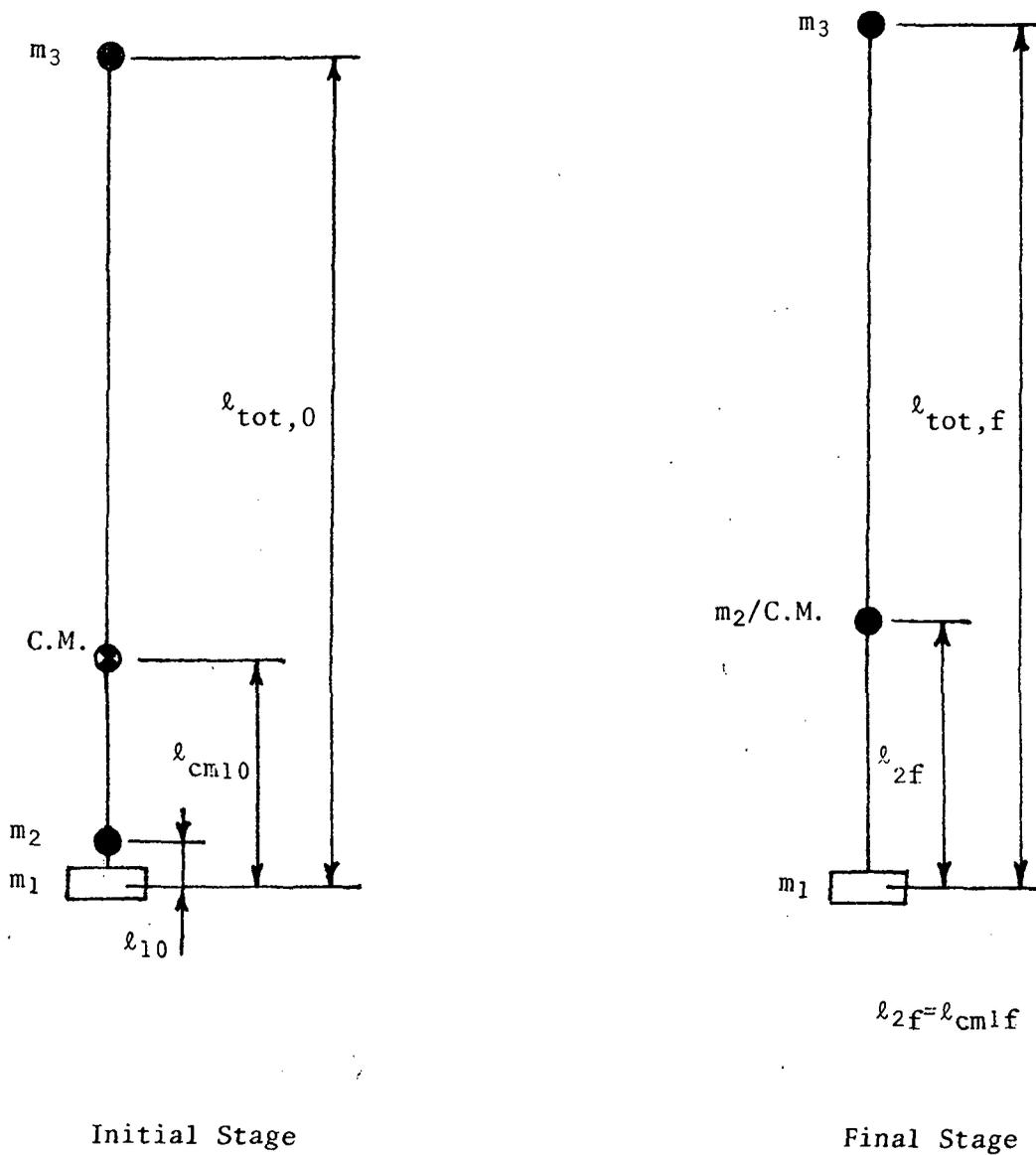
Figure 2.1.1

$m_{eq1,3} = m_1 m_3 / (m_1 + m_3)$. ℓ_{c10} and ℓ_{c20} are respectively given by:

$$\ell_{c10} = \frac{\ell_{10}}{1 + 2\, T_{10}/(EA)}$$

$$\ell_{c20} = \frac{\ell_{tot,0} - \ell_{10}}{1 + 2\, T_{20}/(EA)}$$

(2.1.5)

where T_{10} and T_{20} are the initial tension in tether #1 and tether #2, which are respectively given by:

$$T_{10} = 3\Omega^2 m_1 \, \ell_{CM10}$$

(2.1.6)

$$T_{20} = 3\Omega^2 m_3 \, (\ell_{tot,0} - \ell_{CM10})$$

In equations (2.1.5) it is assumed that at the beginning of the maneuver we have $\ell_{1d} = \ell_{1t}$ and $\ell_{2d} = \ell_{2t}$, where ℓ_{1d} and ℓ_{2d} are the damper lengths for damper #1 and #2 respectively, while ℓ_{1t} and ℓ_{2t} are the tether stretches for the associated tether segments. The conditions $\ell_{1d} = \ell_{1t}$ and $\ell_{2d} = \ell_{2t}$ imply that the longitudinal dampers are tuned to the longitudinal tether frequencies at the initial tether lengths. It will be shown later on that this is true during the entire maneuver because of the adaptive control logic adopted, in this particular simulation, for the longitudinal dampers.

The initial distance between the system C.M. and m_1 is given by:

$$\ell_{CM10} = \frac{m_3 \ell_{tot,0} + m_2 \ell_{10}}{m_{tot}}$$

(2.1.7)

The last unknown quantity in equation (2.1.2) is the final tension in tether #1 that is given by:

$$T_{1\ell} = 3\Omega^2 m_{eq1,3} \; \ell_{tot,\ell} \qquad\qquad (2.1.8)$$

We can therefore compute the value of $\Delta\ell_c$ on the basis of the initial geometry and masses of the constellation. In the present simulation, with the platform masses as shown in Quarterly Report #3, an initial length for tether #1 ℓ_{10} = 10m and an initial overall length of the constellation $\ell_{tot,0}$ = 10 km we obtain $\Delta\ell_c$ = 302.041 m. This simulation has been run in a way slightly different from the simulations reported in the previous quarterly report. A station-keeping phase (no displacement of the middle mass) of 1000 sec precedes the maneuver in order to reduce the effect of imperfect initial conditions. Moreover the longitudinal dampers are adaptive: the gains are varied with time in such a way that the damper is constantly tuned to the associated tether longitudinal frequency (it changes with length) and the damping coefficient is .9. Nevertheless, it is evident from the results shown in Figure 2.1.2 a-i that the 1000 sec station-keeping phase is not long enough to damp out completely the initial longitudinal oscillations. No further investigation, however, has been performed on this peculiar station-keeping phase characterized by a very short tether length for tether #1 and high frequency longitudinal oscillations. Figure 2.1.2a shows the length variation of tether #1 vs. time. The initial station-keeping phase and the smooth start of the maneuver are clearly shown in the figure. The longitudinal damper tether length for tether #1, shown in Figure 2.1.2.b, has the same shape as the tether length variation because the damper is adaptive. Figures 2.1.2c and d show the in-plane angle vs. time and the θ-$\dot{\theta}$ phase plane respectively. The θ variation is very small and a small residual angular velocity is still present at the end of the simulation. This residual velocity would be damped out completely in a longer simulation run. The lateral deflection of the middle mass ϵ vs. time is shown in Figure 2.1.2e while the phase plane ϵ-$\dot{\epsilon}$ is shown in Figure 2.1.2f. It is evident from these figures that the ϵ oscillation

is perfectly damped out at the end of the simulation. Figures 2.1.2g and h show the vertical and the horizontal component respectively of the acceleration meas- ured at the middle mass. As mentioned before, the transient oscillations due to imperfect initial conditions are not completely abated at the end of the sta- tion-keeping phase. It is possible that the delay introduced by the numerical integration in adjusting the frequency of the longitudinal damper to the longi- tudinal oscillation frequency has a role in the transient response during sta- tion-keeping. Since the delay is comparatively more significant at high-fre- quency (short tether length) than at low frequency it is plausible that these transient oscillations disappear when the tether is lengthened. All these hy- potheses have not been verified because the initial transient response does not affect the final steady state. The two above mentioned figures show clearly that the acceleration components at the end of the run go to zero as expected. Note that a perfect zero condition at the end of the simulation run is due to the absence of steady state perturbations (e.g. J_2 gravity term and air drag) in this simulation. Figure 2.1.2i shows the tension of tether #1 vs. time while the tension in tether #2 is not shown because it is of no significance.

As a conclusion to this "zero-g-tuning" simulation we must point out that this simulation run can be also viewed as an alternative deployment strategy of the 3-mass constellation. In the alternative deployment sequence the end mass is deployed from the Space Station following a conventional deployment maneuver, for example, like the one adopted for the TSS satellite. Subsequently the middle mass is moved along the tether from the Space Station to the zero-g point of the system according to the strategy explained above.

A possible improvement to the control law developed in this section is the development of a closed loop control law in which the distance between the middle mass and the system C.M. is fed back into the control law. This modifi-

ORIGINAL PAGE IS
OF POOR QUALITY

Figure 2.1.2a↑

Figure 2.1.2b↓

IN-PLANE ANGLE (Deg)

TIME (Sec)   Rotat. + Longit. Dampers

Figure 2.1.2c↑

Figure 2.1.2d↓

THETAD (Deg/Sec)

END

START

THETA (Deg)   Phase Plane
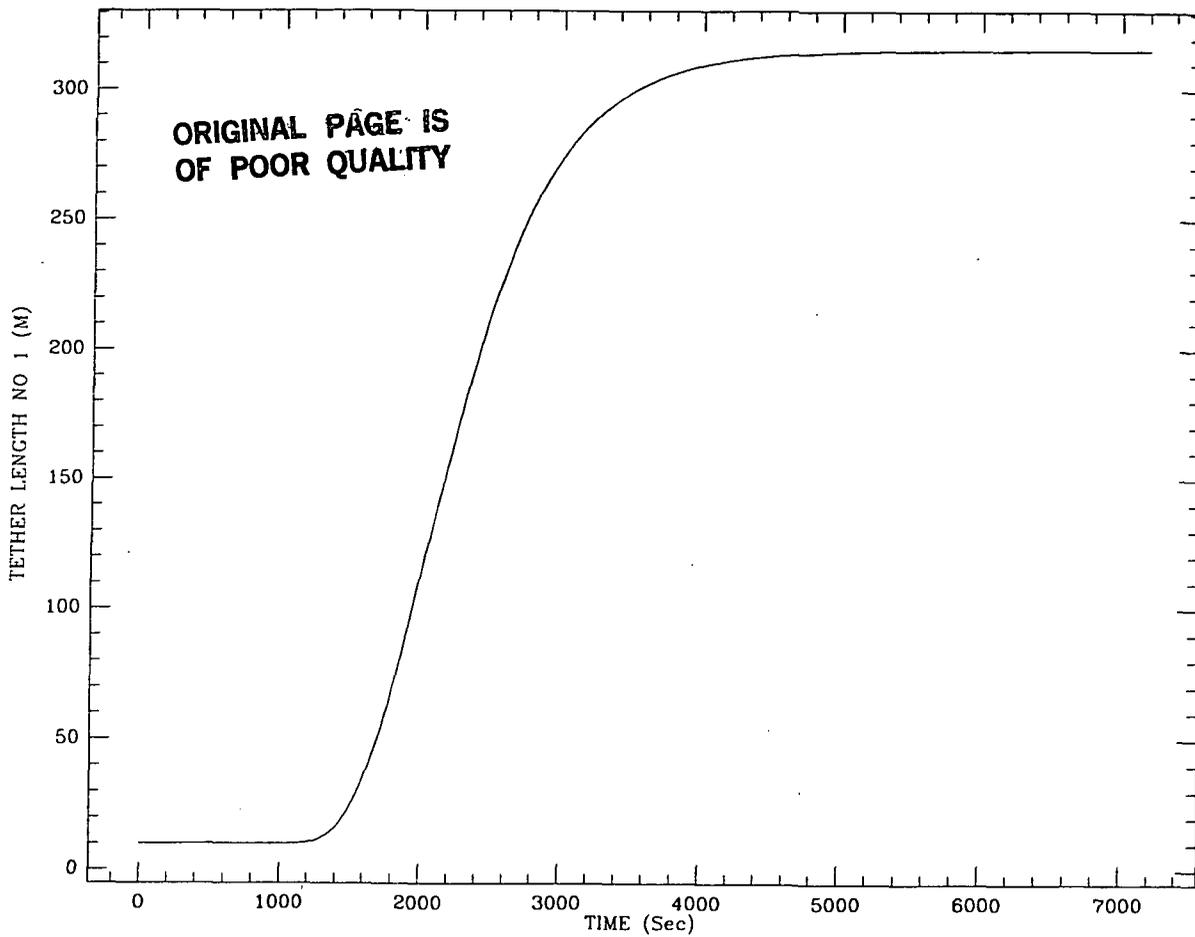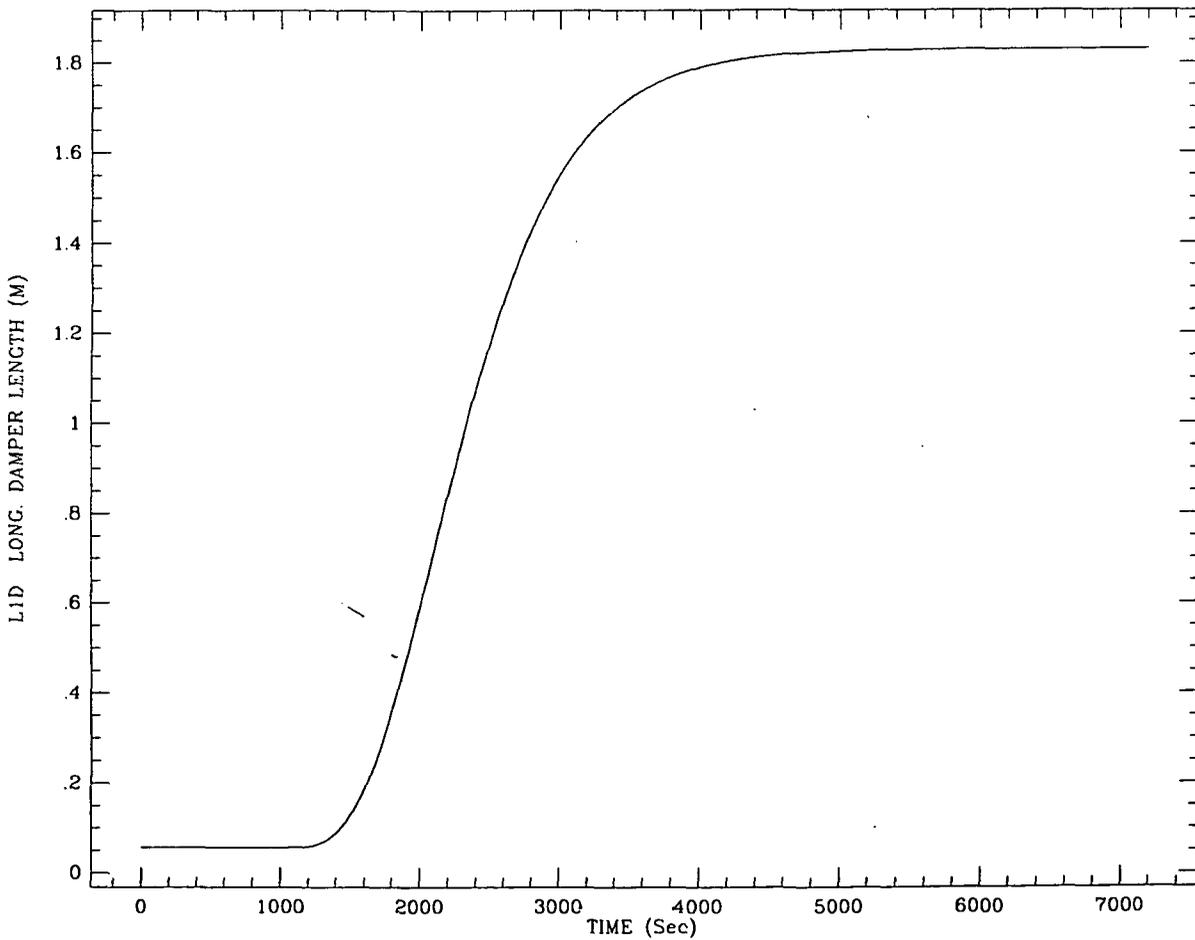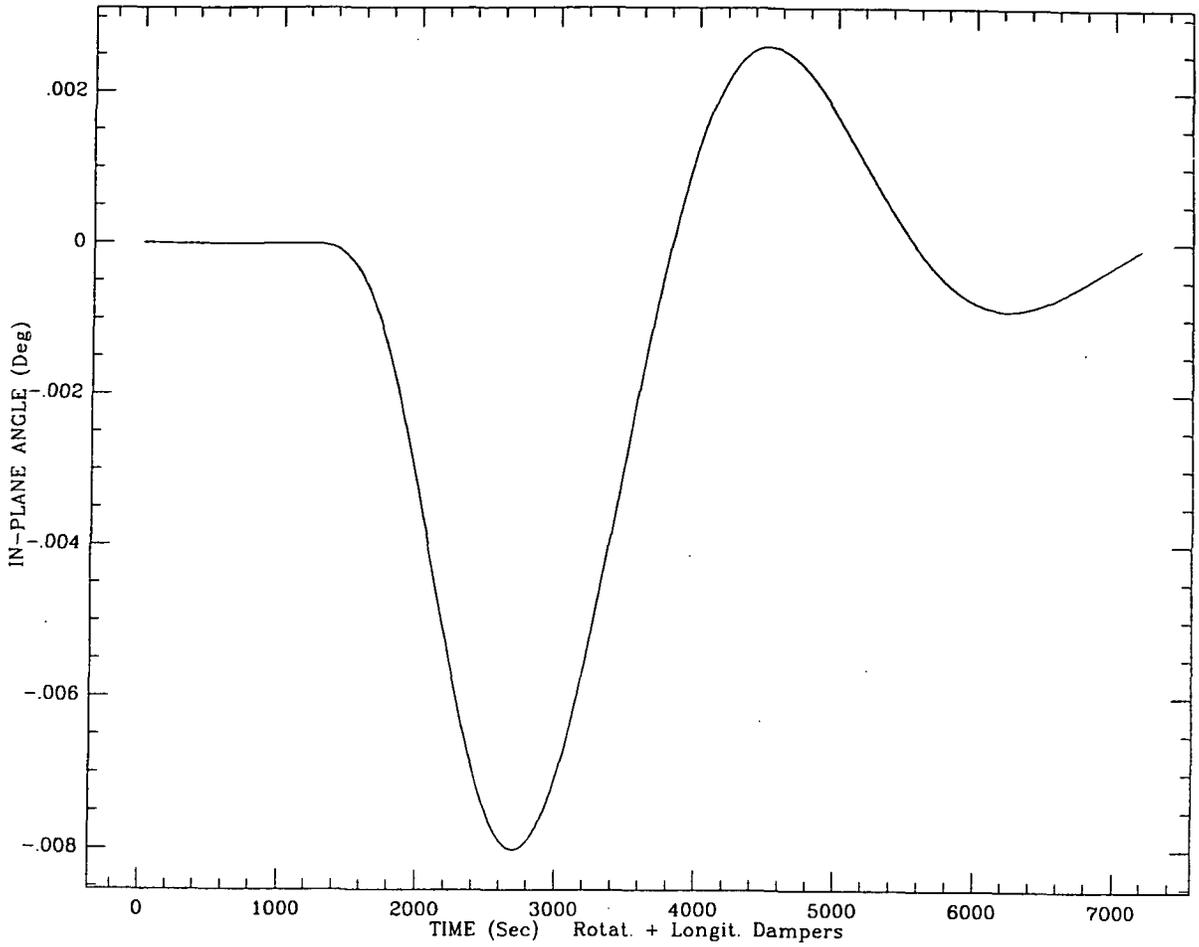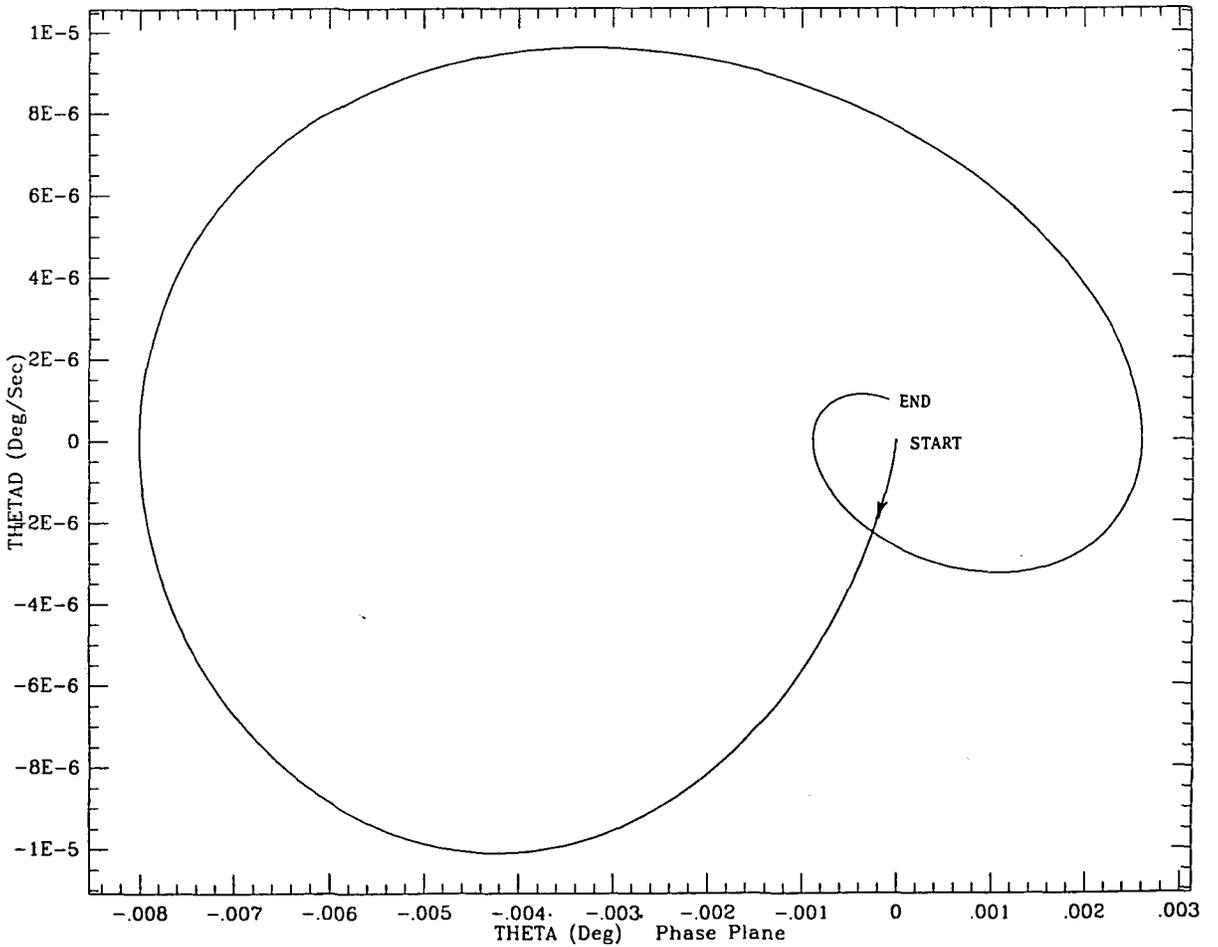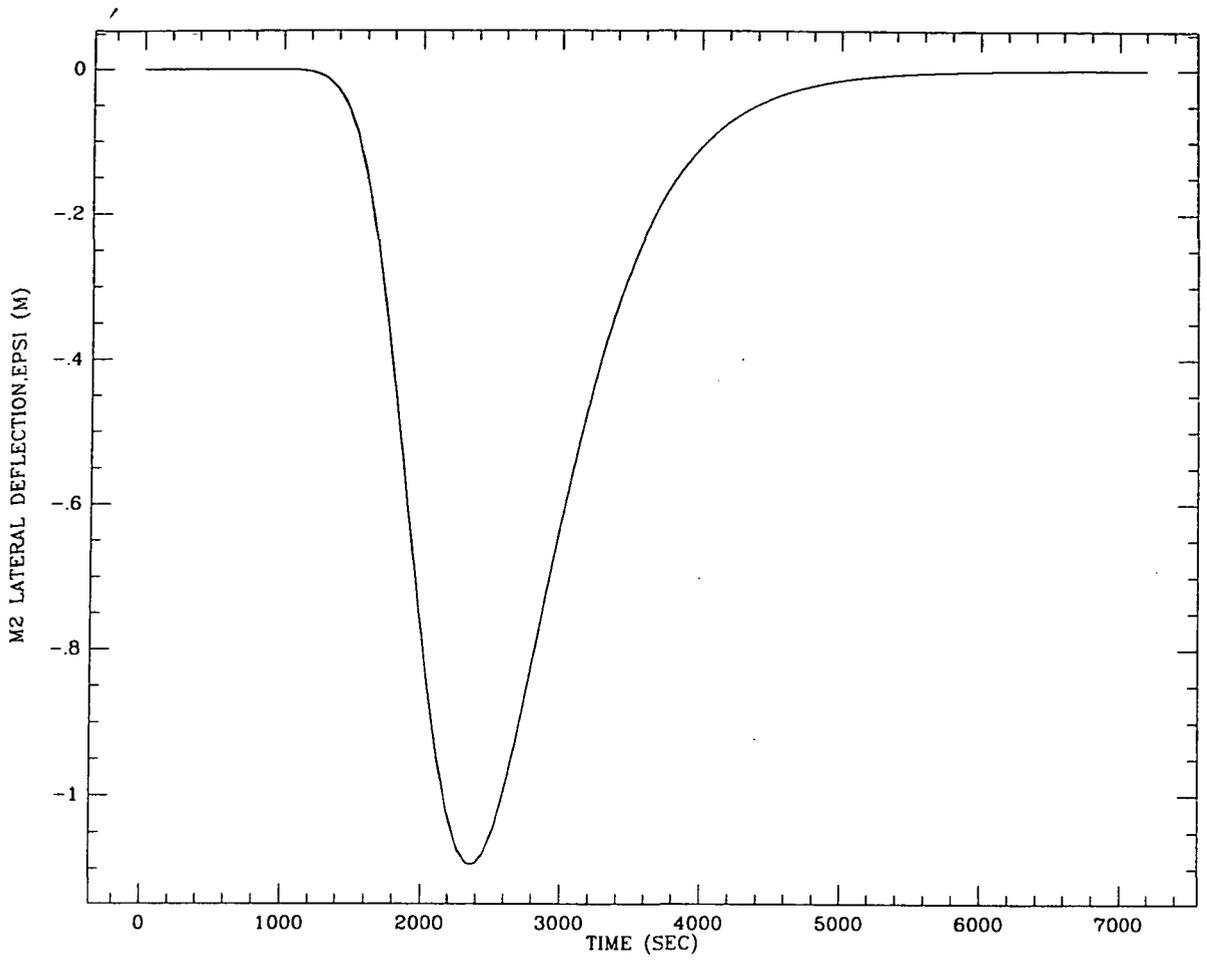
Figure 2.1.2e↑
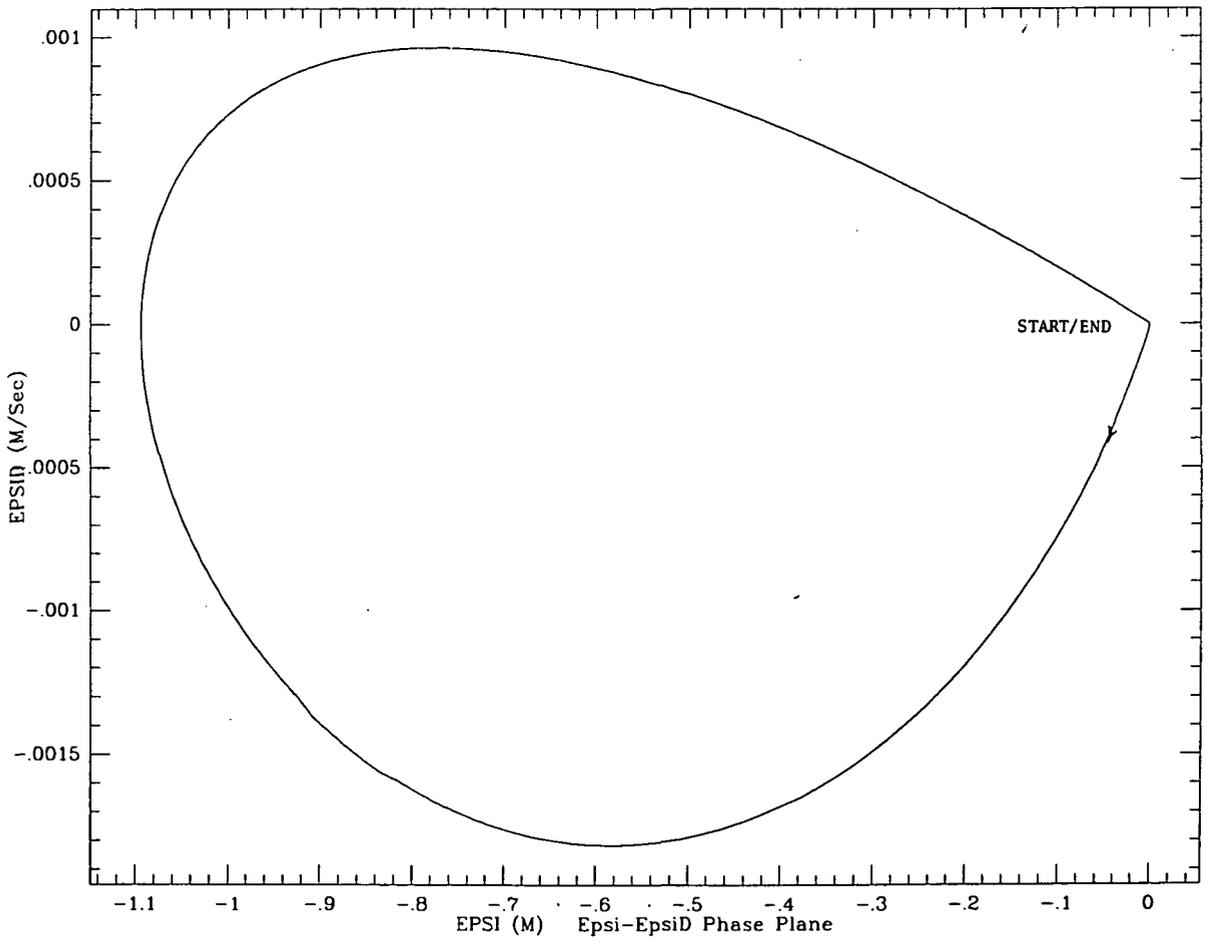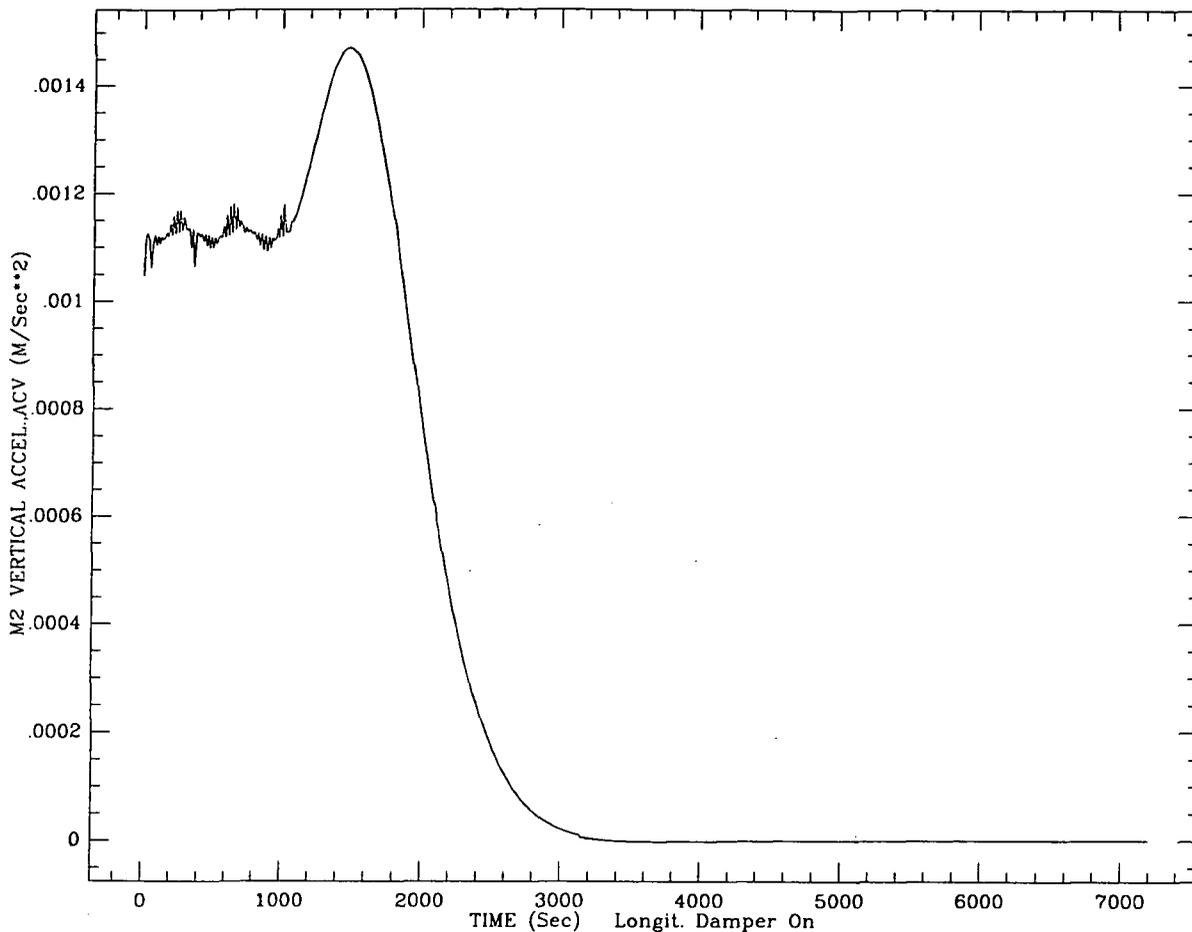
Figure 2.1.2f↓

Figure 2.1.2g↑

Figure 2.1.2h↓
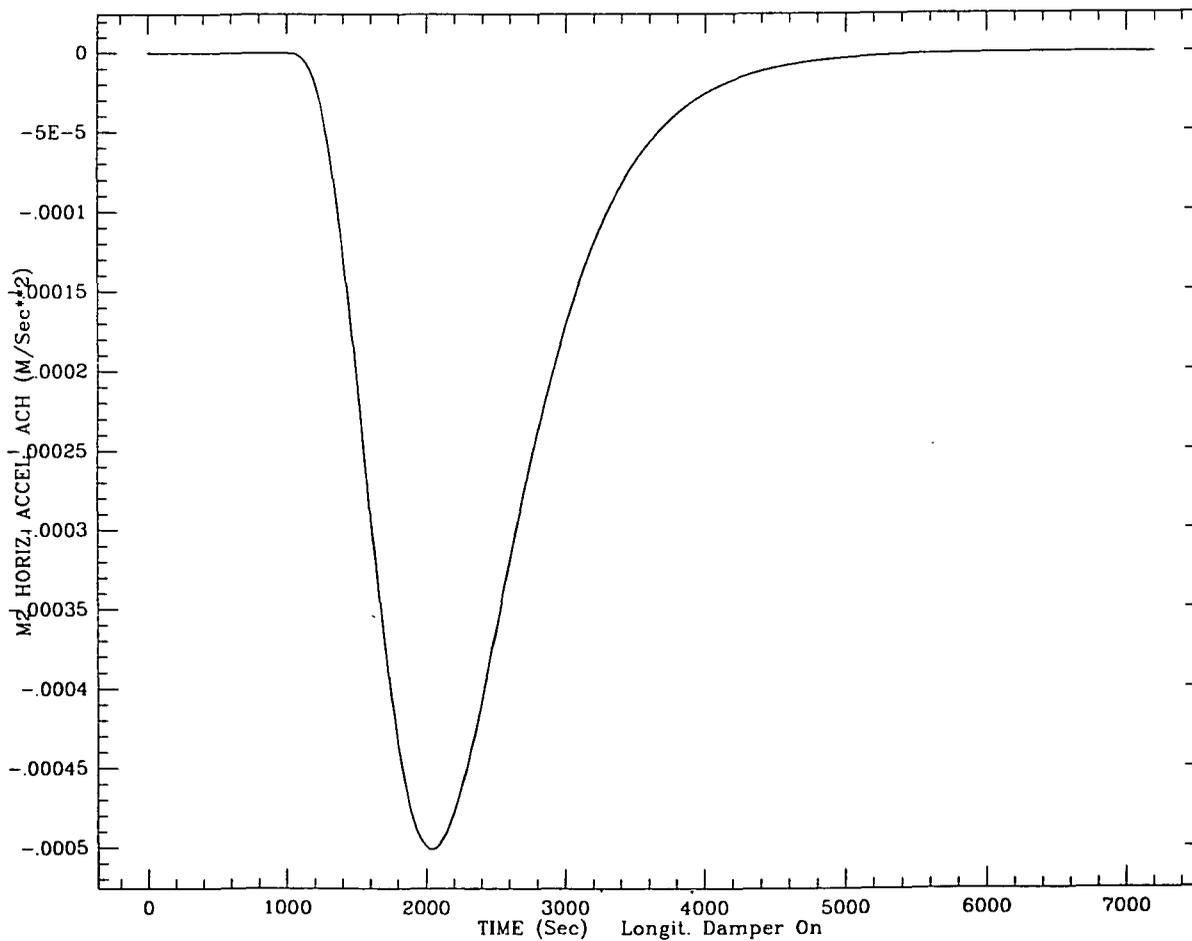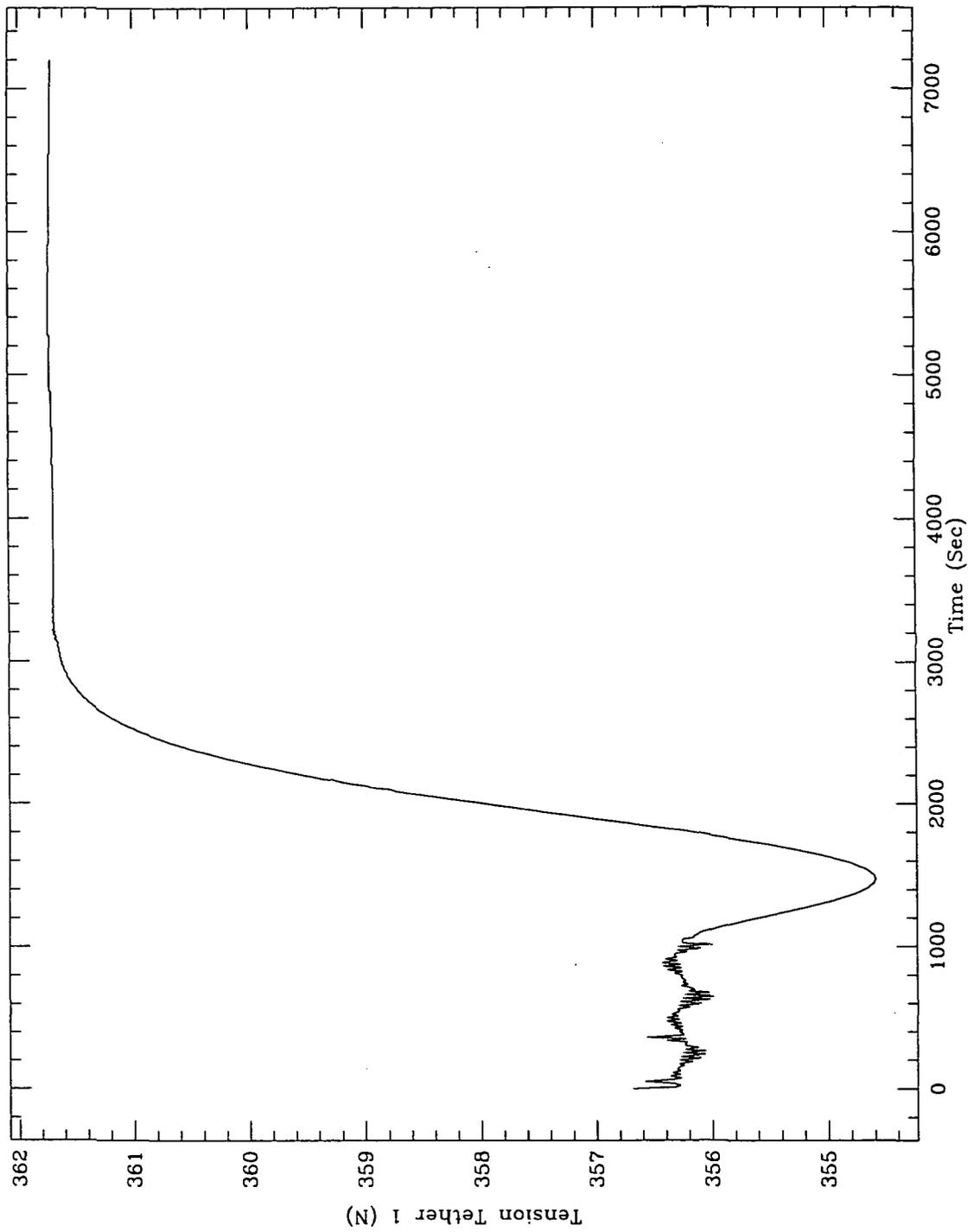
Figure 2.1.2i

cation makes the system response more insensitive to perturbations.

2.2 Middle Mass Travelling From One Tether End To The Other

The middle mass of a 3-mass vertical tethered constellation can be used to service the end mass. In this application the middle mass is moved from the Space Station to the end mass and vice versa in order to transfer materials between the two platforms. In this section the motion of the middle mass from the Space Station to the end mass is analyzed. This case is the most critical of the two from the point of view of the instabilities which take place when the middle mass approaches the end body since the end mass is less massive than the Space Station. The control law adopted in this maneuver is like the one represented in equations (2.1.1) of the previous section. The procedure for computing the value of the length variation $\Delta \ell_c$ is also similar to the one described in the previous section if the distance from mass #1 to the final position of the system's center of mass ℓ_{CM1F} is replaced by the distance between mass #1 and the final position of the middle mass ℓ_{2f}. Two cases have been analyzed: in the first case the longitudinal dampers are adaptive while in the second case the dampers are non-adaptive. Both simulations start with an initial tether length for tether #1 equal to 10m. An initial tether length different from zero accounts for a deployment boom between the middle mass and the Space Station; at the same time it makes possible the efficient integration of the equations of motion at the start of the simulation. The longitudinal oscillation frequency is in fact dependent upon the tether length and increases to infinity for zero tether length. In both simulations the value of the time constant $1/\alpha$ for the hyperbolic tangent control law is 2000 sec while the exponent γ has been assumed equal 4. In the non-adaptive case the longitudinal dampers are tuned to the

average tether length of 5000 m. Therefore the dampers have the best efficiency
when the middle mass is crossing the mid-way point between the Space Station and
the end mass. In both simulations the maneuver is preceded by a station-keeping
phase of 1000 sec in order to abate the transient motion due to imperfect ini-
tial conditions. However, since the non-adaptive longitudinal dampers are inef-
ficient for short tether lengths the abatement of the oscillations due to the
initial conditions is better in the case of the adaptive control. The dynamic
response of the system in the case of the adaptive control is shown in Figures
2.2.1a-m. Figure 2.2.1a shows the tether length variation of tether #1 vs.
time. The tether length variation of tether #2 is the complement to the total
tether length. Figure 2.2.1b shows the tether velocity of tether #1 vs. time
while Figure 2.2.1c depicts the length variation of the longitudinal damper
associated to tether #1. Since the damper is adaptive, its length variation is
proportional to the associated tether length variation. Figure 2.2.1d and e
show respectively the in-plane angle of the constellation vs. time and the phase
plane θ-$\dot{\theta}$. Both figures indicate that the overall in-plane oscillation is very
stable and well damped during the maneuver. The maximum in-plane angle does not
exceed 3.5°. Figures 2.2.1f and g depict the lateral deflection (ϵ) of the
middle mass with respect to the line through m_1 and m_3 vs. time and the phase
plane ϵ-$\dot{\epsilon}$ respectively. We can conclude that the lateral oscillation ϵ is also
very stable and well damped. The damping is provided by the feed-back control
loop associated with the reeling mechanism. Figures 2.2.1h and i represent the
vertical and horizontal component respectively of the acceleration measured on
board the middle mass. It is evident from these two plots that the vertical
acceleration component of the middle mass reaches the value consistent with the
final offset from the system C.M. while the horizontal acceleration component,
perturbed from rest conditions by the middle mass motion, tends to zero at the
end of the maneuver. Figures 2.2.1j and k show the tension in
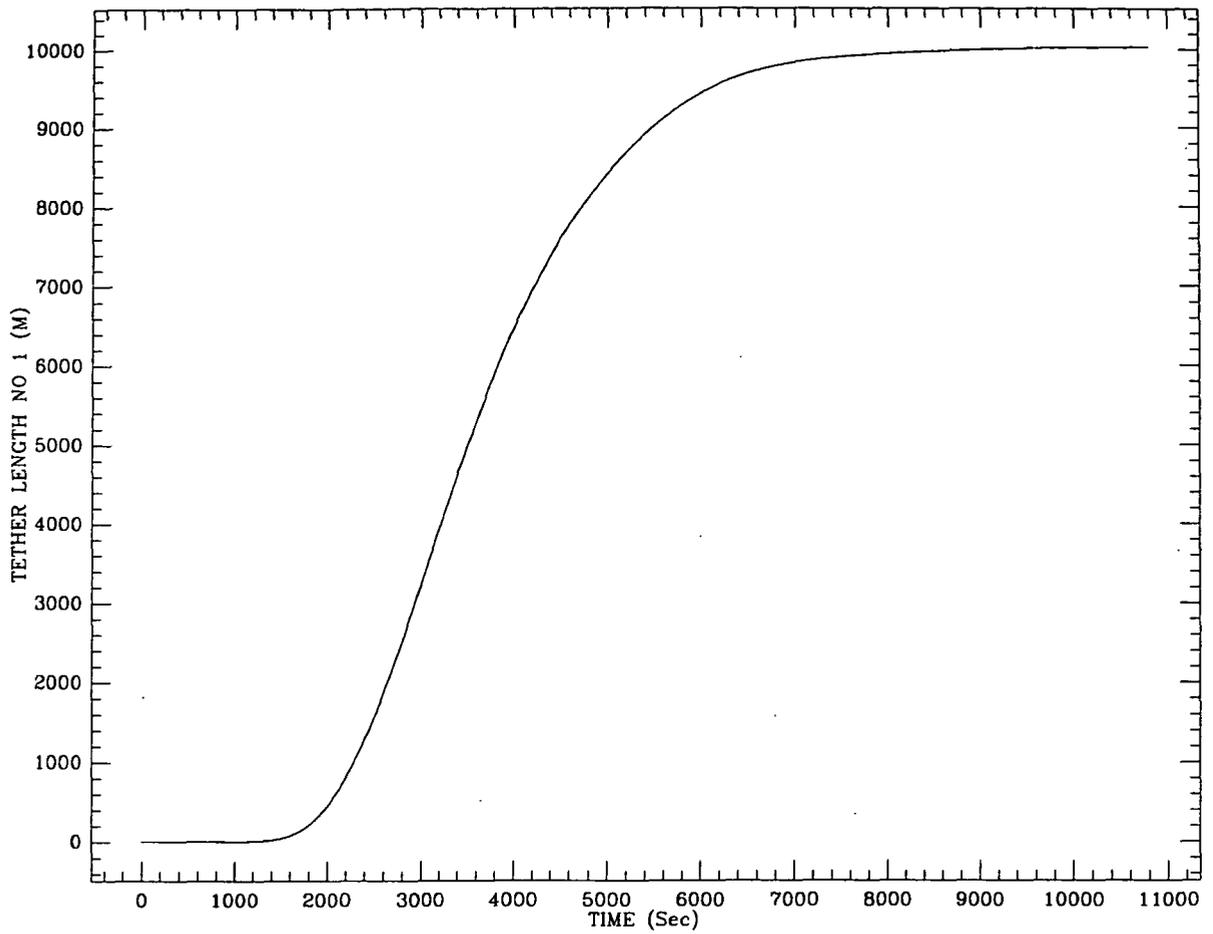
Figure 2.2.1a↑

Figure 2.2.1b↓
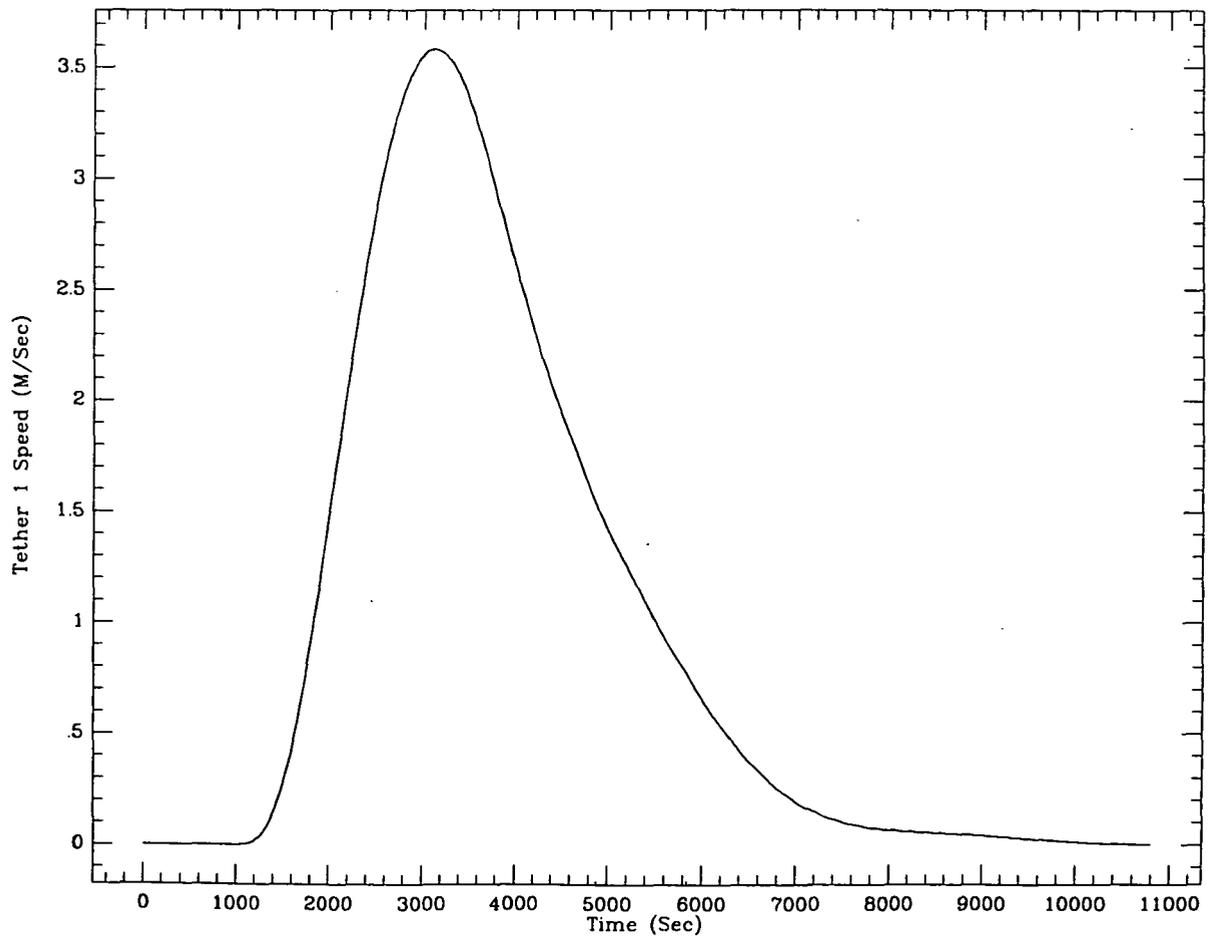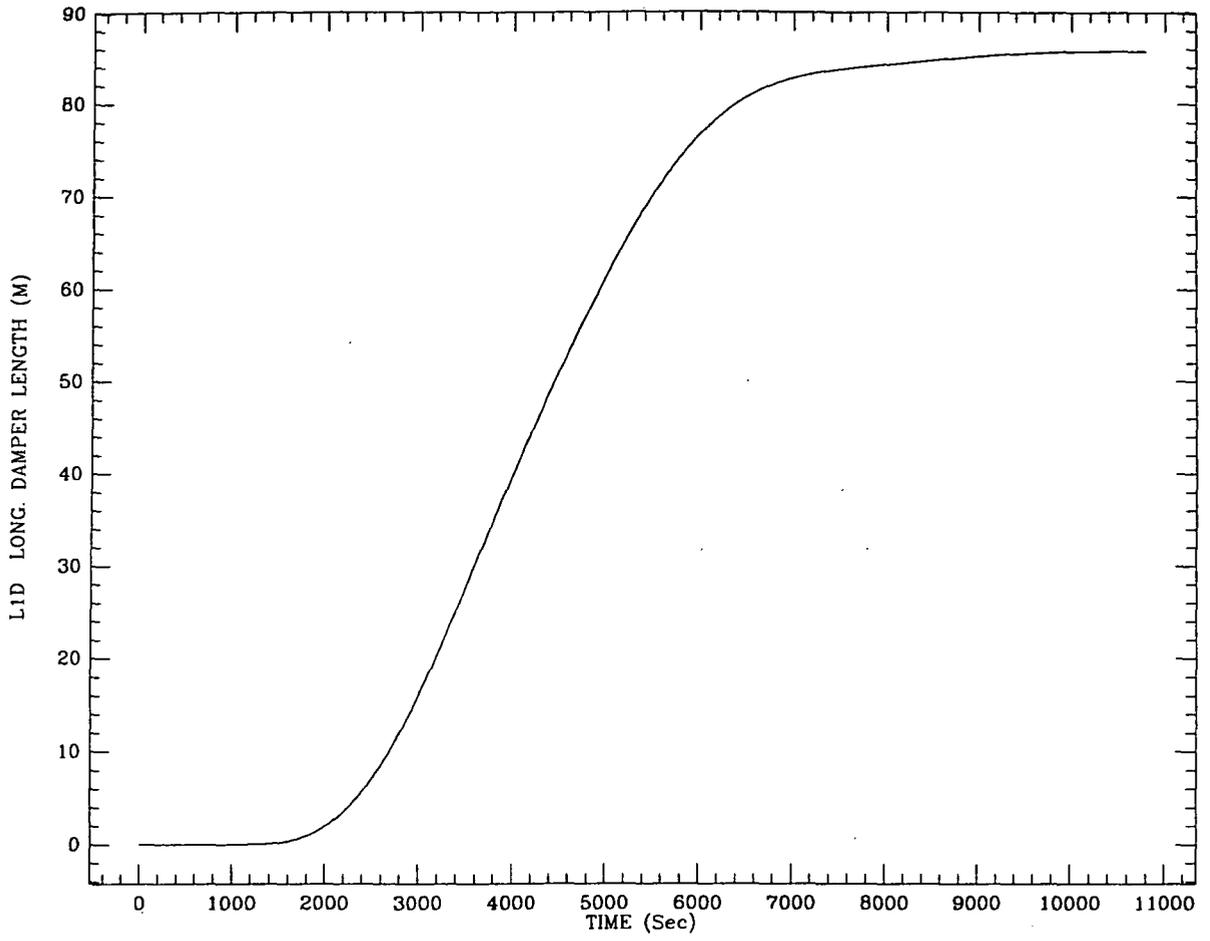
Figure 2.2.1c↑

Figure 2.2.1d↓
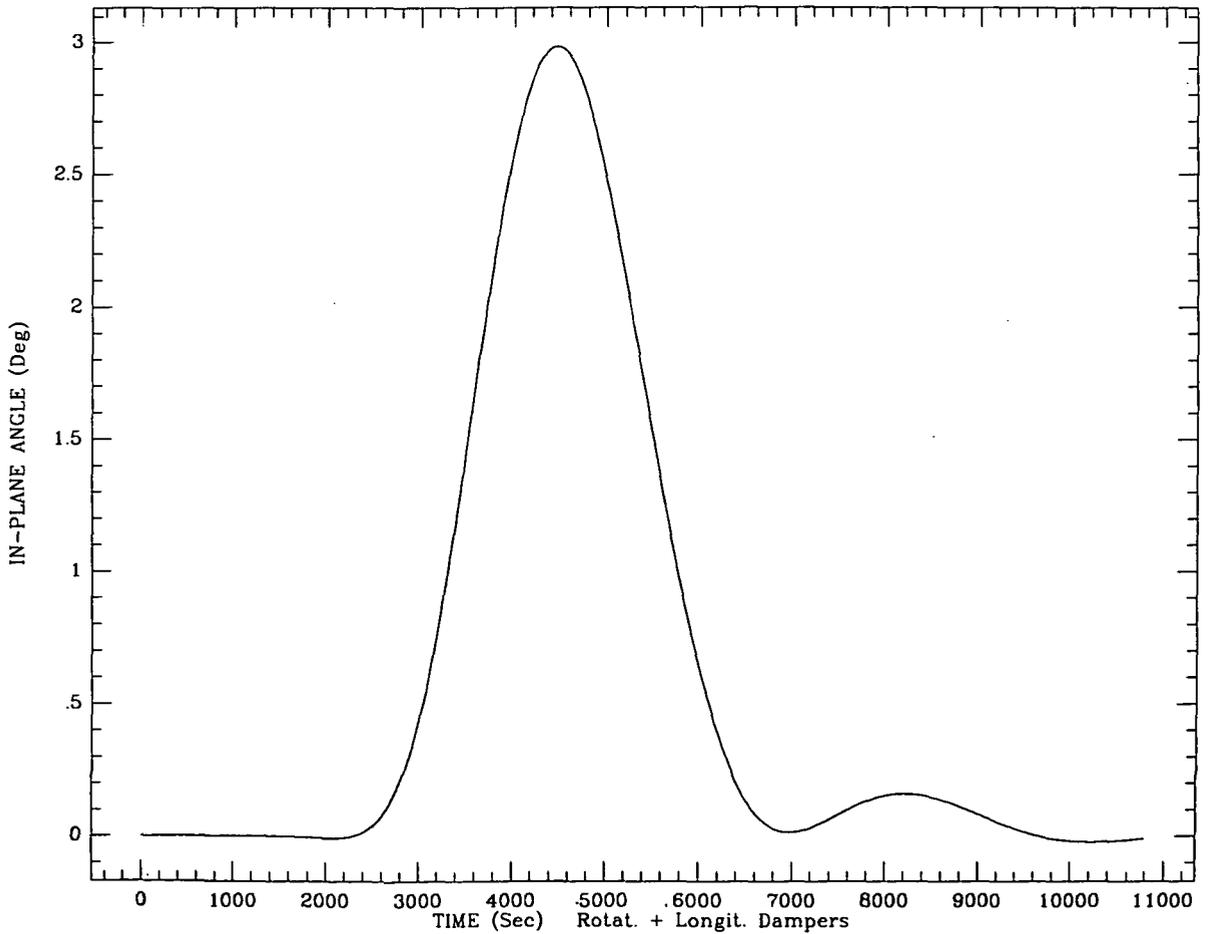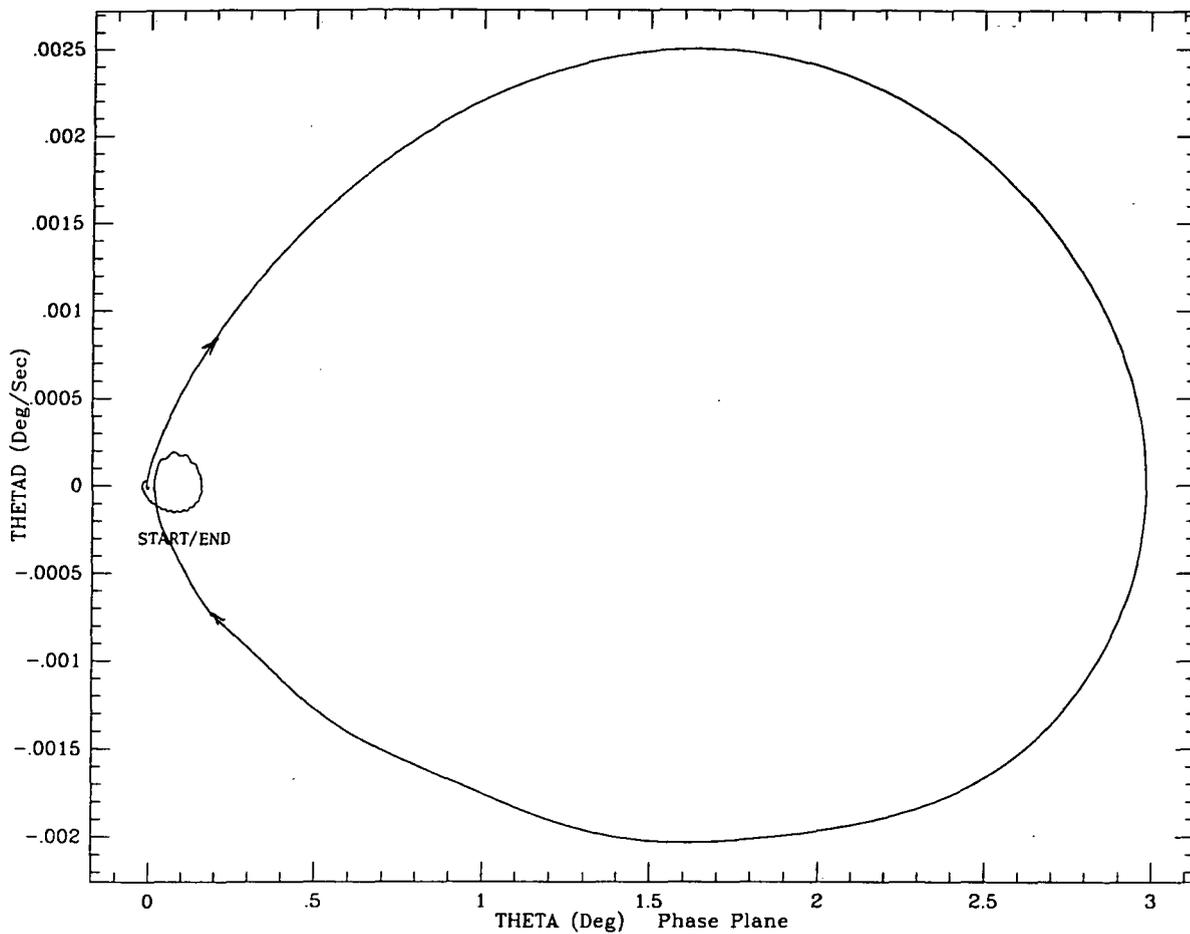
Figure 2.2.1e↑

Figure 2.2.1f↓
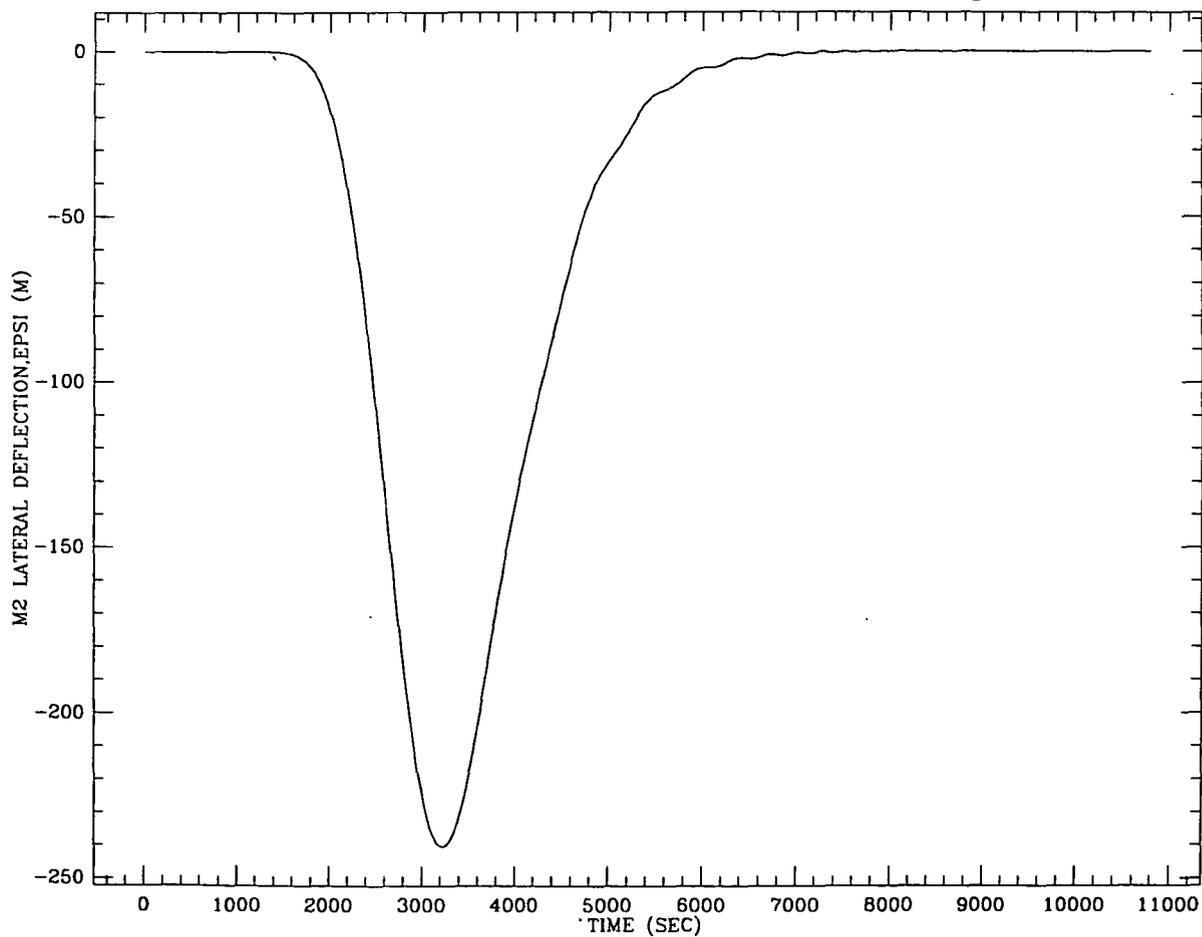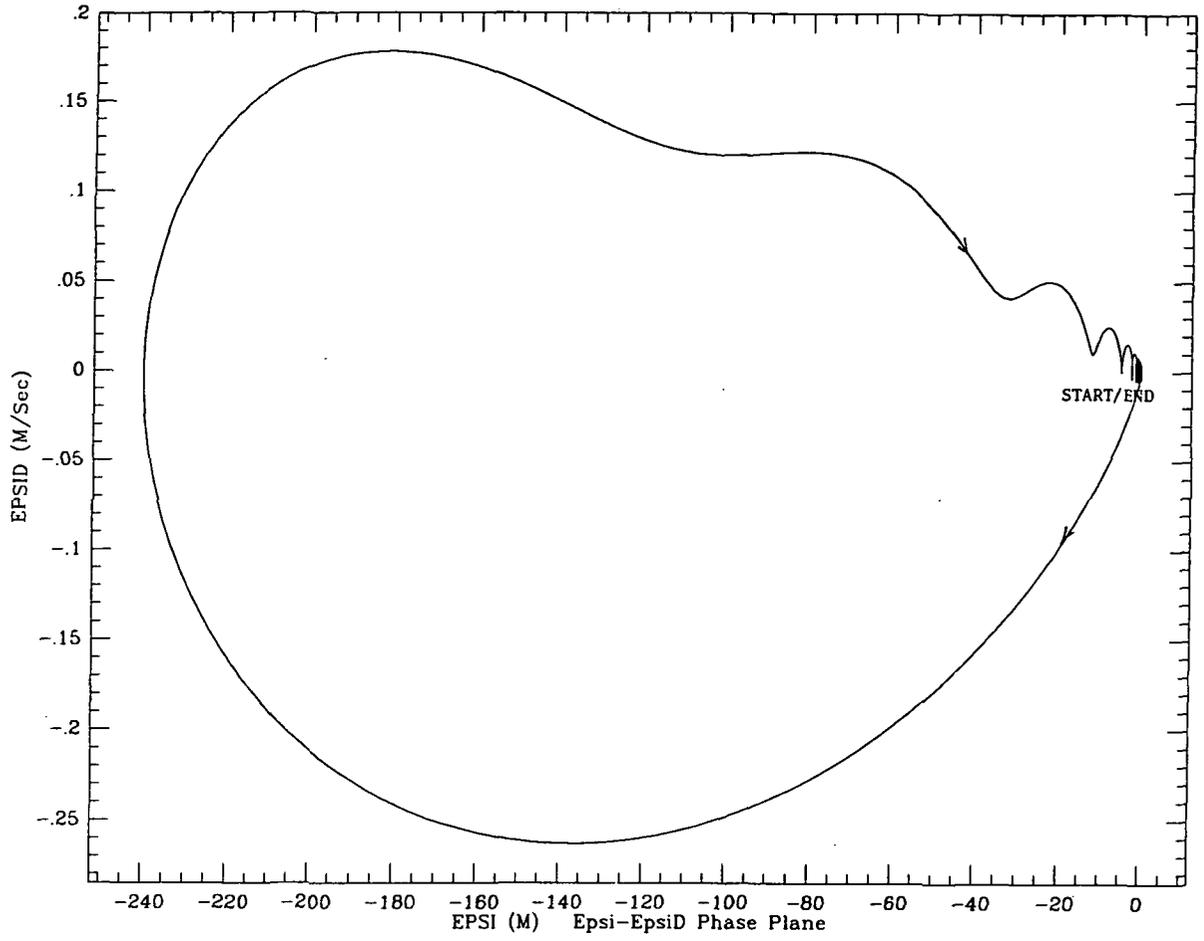
Figure 2.2.1g↑

Figure 2.2.1h↓
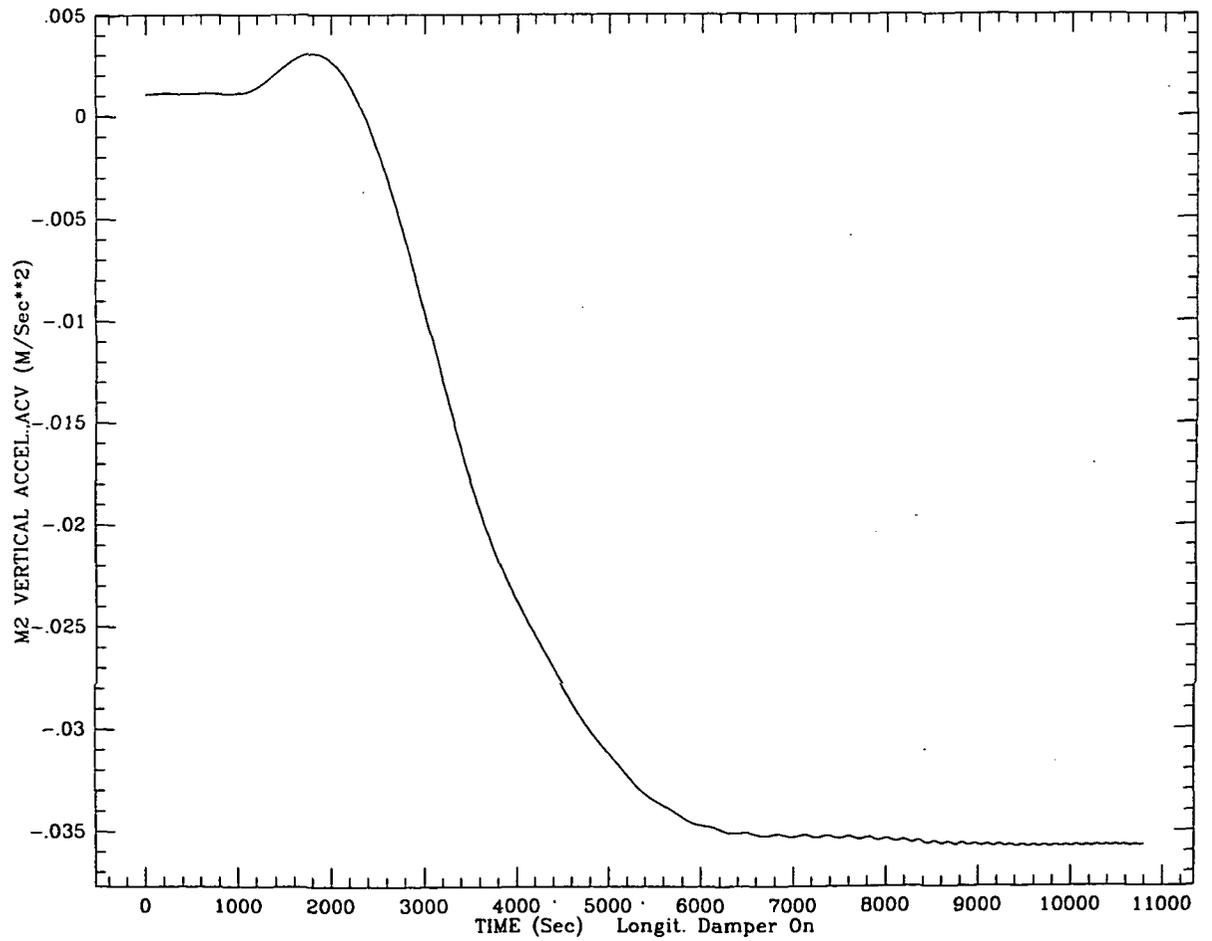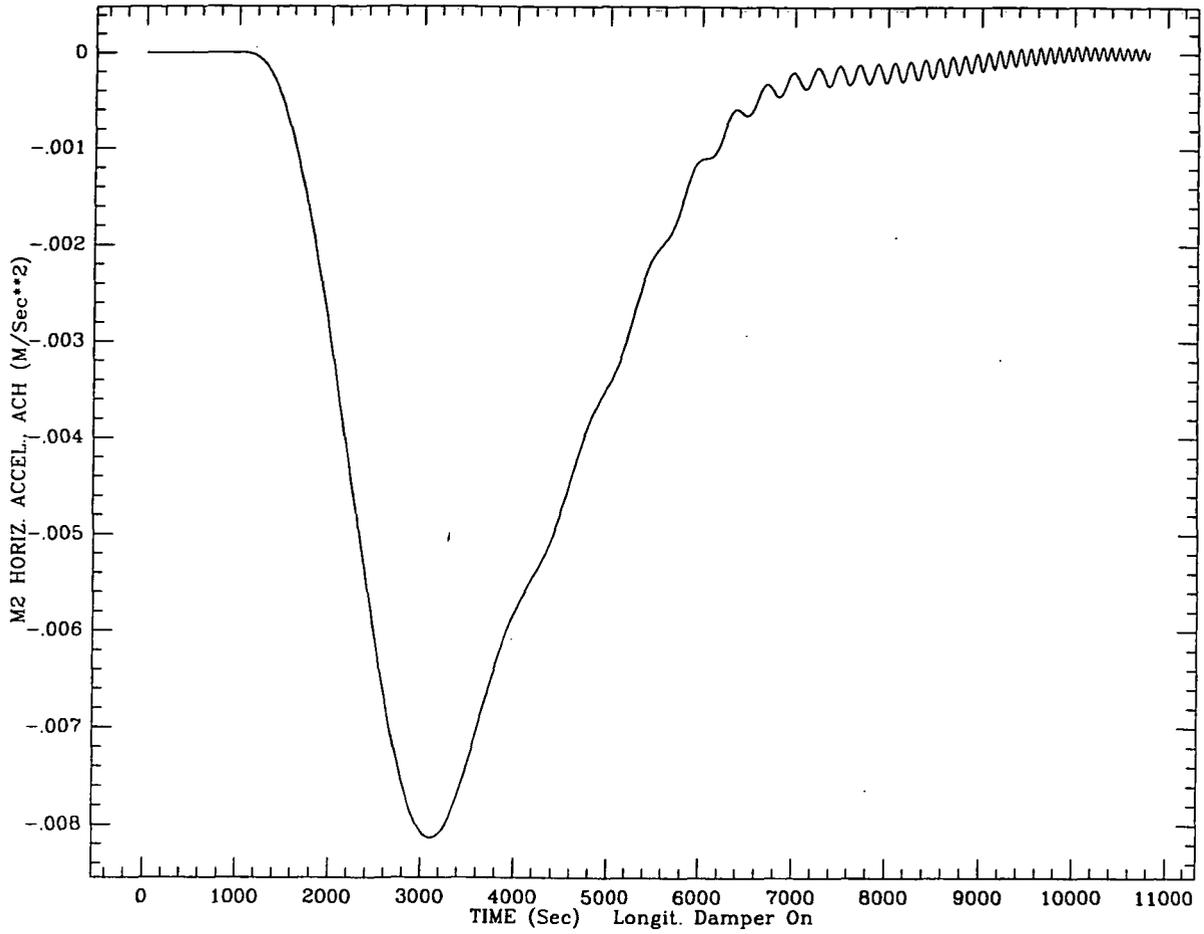
Figure 2.2.1i↑

Figure 2.2.1j↓
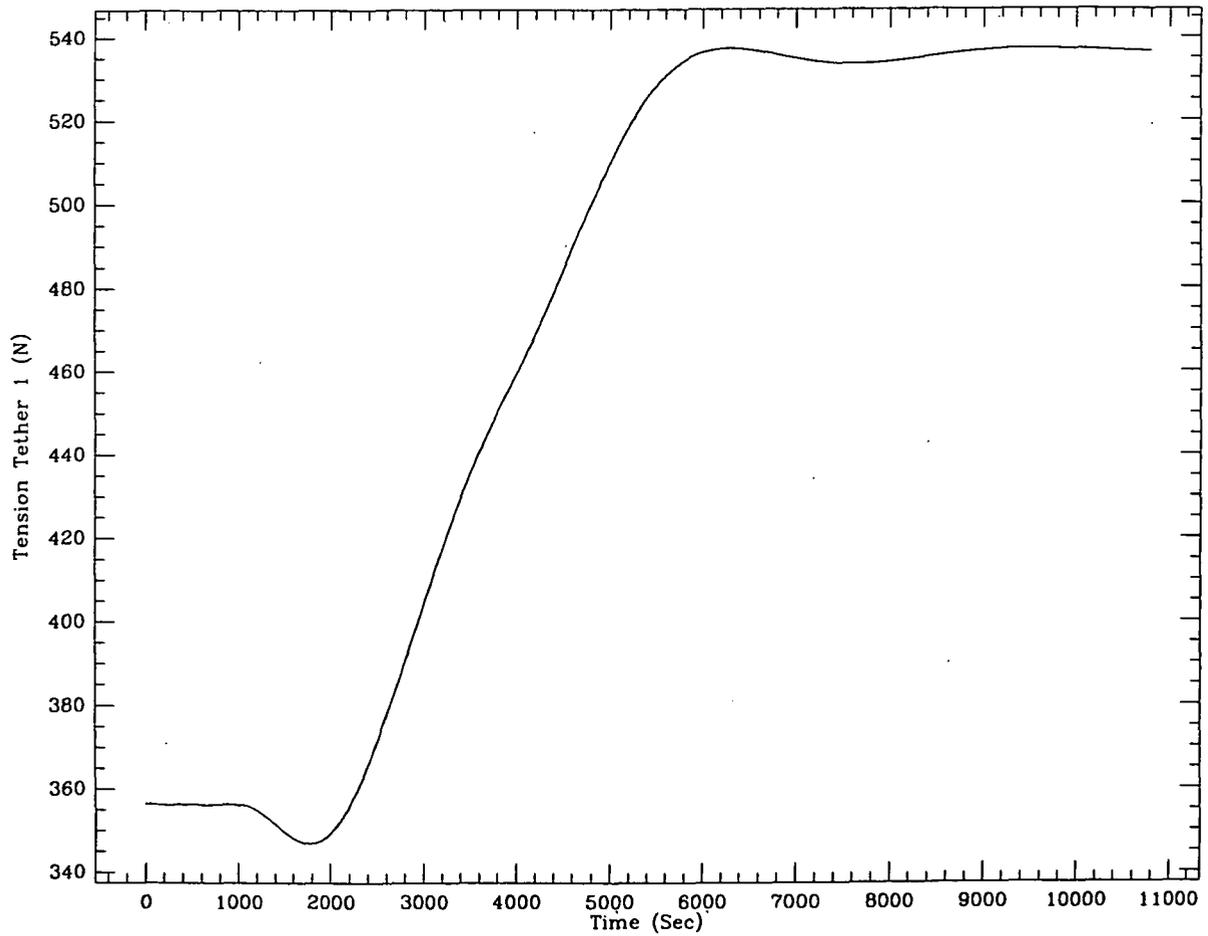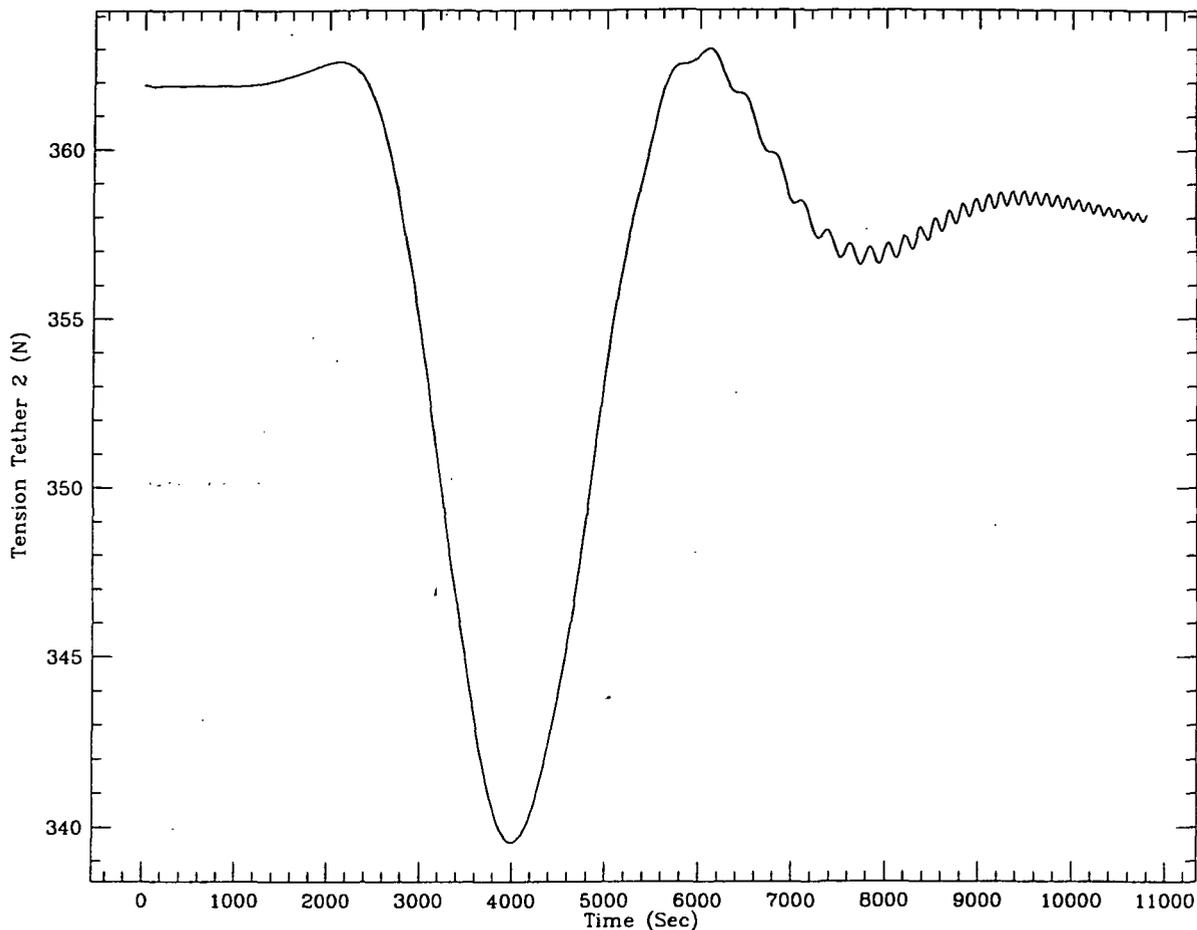
Figure 2.2.1k↑

Figure 2.2.1ℓ↓
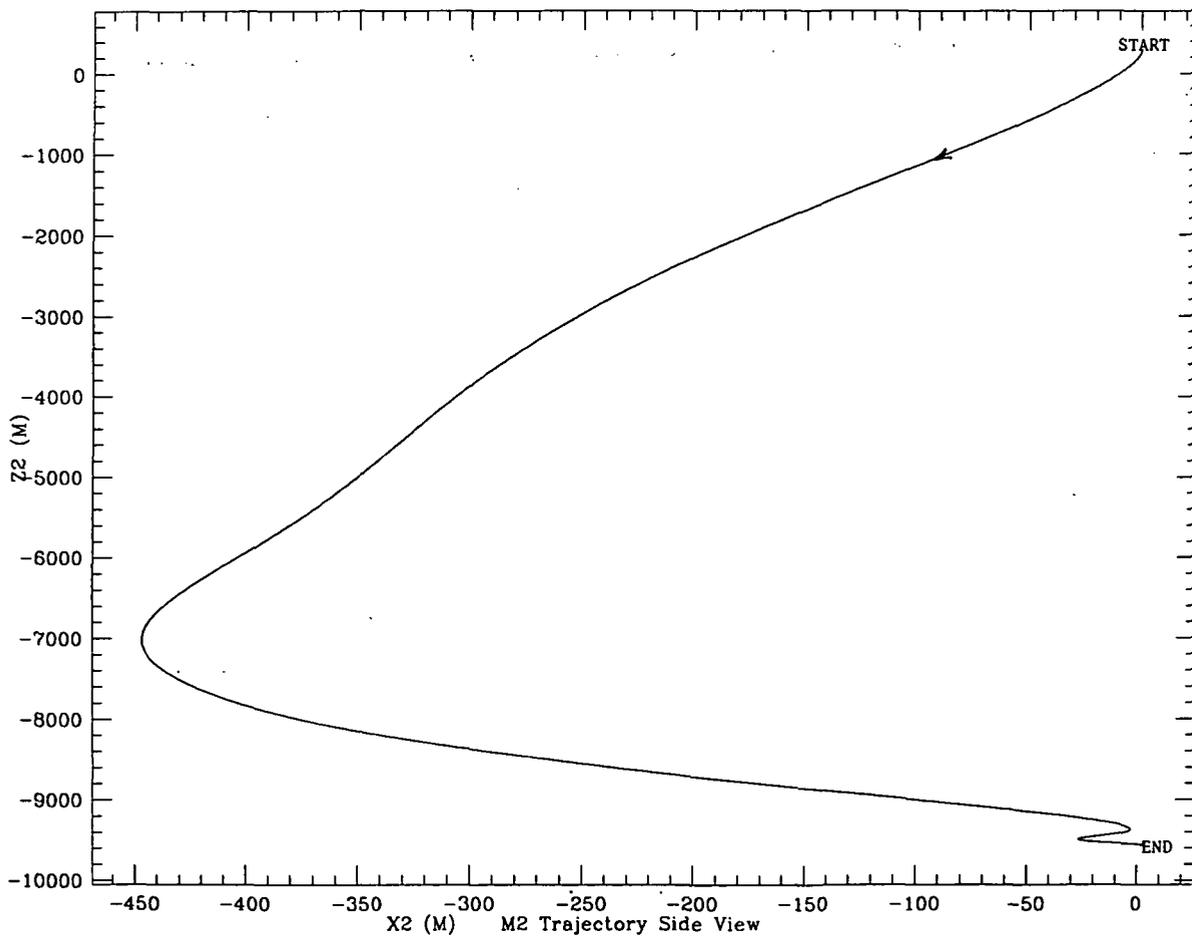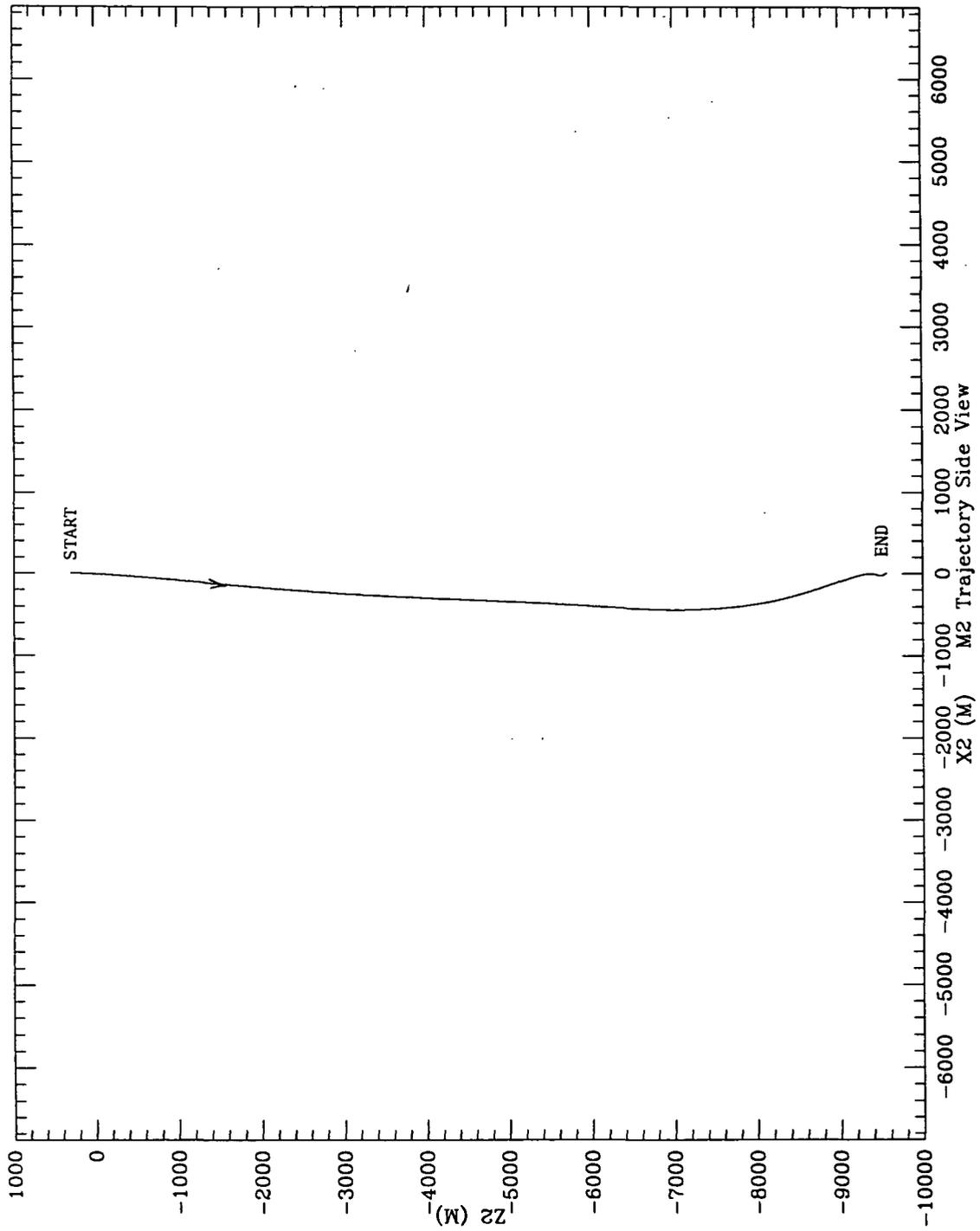
Figure 2.2.1m

tether #1 and tether #2 respectively. The tension in tether #2 shows clearly the frequency increase of the longitudinal oscillations when the tether length is shortened. Figure 2.2.1ℓ is the expanded side view of the trajectory of the middle mass (a negative z meaning outwards) while Figure 2.2.1m is an isometric plot of the same trajectory.

The simulation without the adaptive control logic is similar to the previous simulation except for the longitudinal oscillations in tether #2. Such oscillations show a tendency to diverge. A comparative plot of the tension in tether #2 is drawn in Figure 2.2.2. In this figure the solid line represents the adaptive case while the dashed line is the non-adaptive case. The two lines do not overlap because of a slight difference in the final tether length at the end of the simulations. However the figure clearly shows the better performance obtained by using the adaptive control logic. In the present simulation the diverging oscillations for the non-adaptive case are not critical because of the relatively slow time constant adopted in the control law that allows enough time for the damper to damp out the oscillations. A faster time constant, however, would create a much more critical situation if a non-adaptive control logic is adopted.
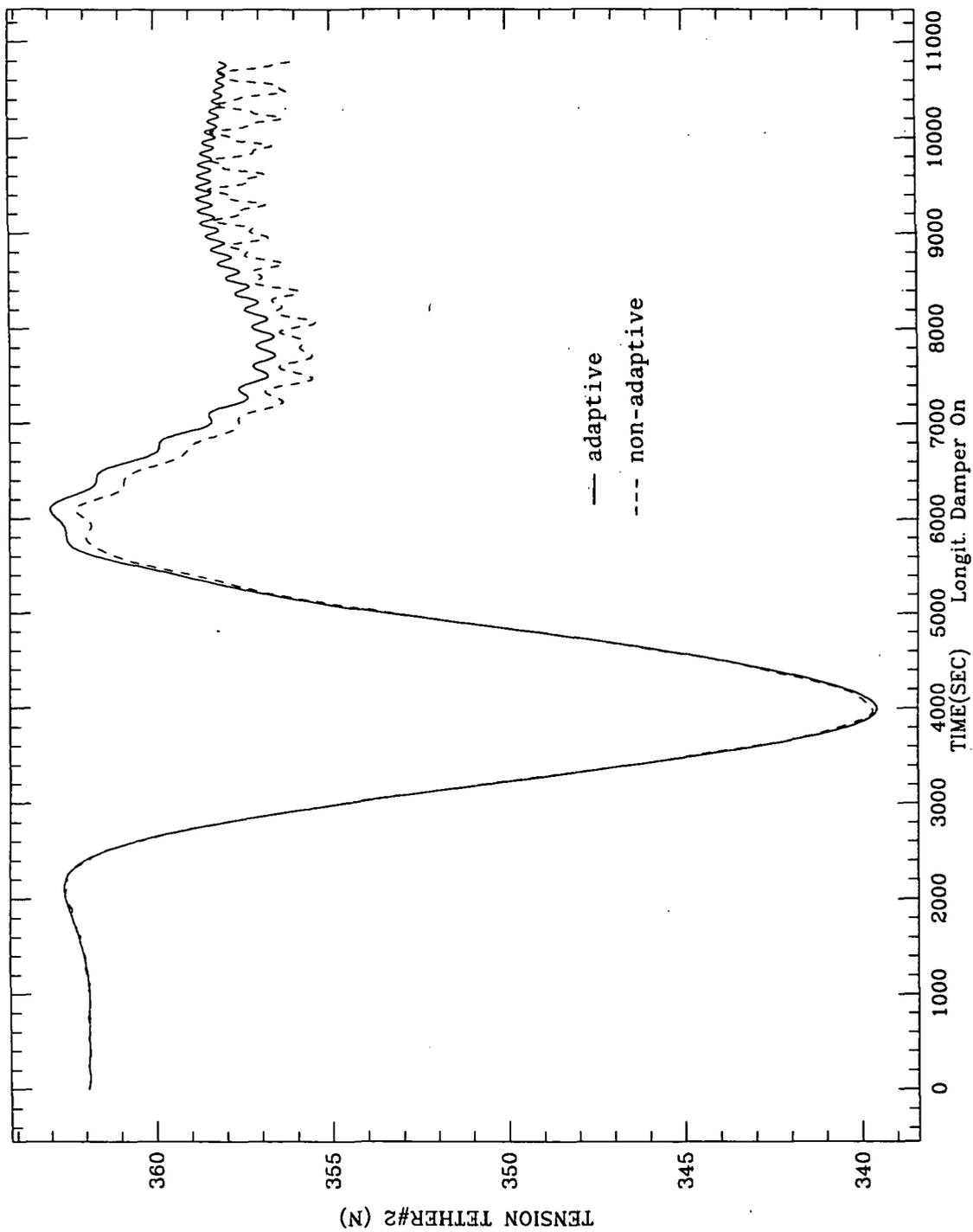
Figure 2.2.2

2.3 Concluding Remarks

The newly modified hyperbolic tangent control law provides the capability for fast and smooth transfer maneuvers of the middle platform along the tether. Two important maneuvers have been dealt with in detail in this report. The first maneuver consists of the achievement of "zero-g" conditions on board the middle mass starting with the middle platform initially in the vicinity of the Space Station. The second maneuver consists of a transfer maneuver of the middle platform from one tether end (Space Station side) to the opposite one. An adaptive control logic has been adopted for the longitudinal dampers. Such control logic is necessary in the second type of maneuvers especially when fast time constants are used in the control law.

3.0 PROBLEMS ENCOUNTERED DURING REPORTING PERIOD

None

4.0 ACTIVITY PLANNED FOR THE NEXT REPORTING PERIOD

In the next reporting period we will initiate the computer implementation of the two-dimensional multi-mass (more than 3) simulation model. Preliminary test cases to check the computer code will also be run if the computer code implementation proceed according to schedule.